Voltage Swell and Overvoltage Compensation With Unidirectional Power Flow Controlled Dynamic Voltage Restorer

Chi-Seng Lam, *Member, IEEE*, Man-Chung Wong, *Senior Member, IEEE*, and Ying-Duo Han, *Senior Member, IEEE*

***Abstract*—Voltage swell and overvoltage compensation problems in a diode-bridge rectifier supported transformerless-coupled dynamic voltage restorer (DVR) are discussed. When swell or overvoltage happens, applying conventional in-phase or phase-invariant boosting method causes a rapid rise in dc-link voltage, which may damage the storage capacitors and switching devices, and increase the switching loss. This paper illustrates the inability of the minimum energy injection scheme to solve these problems during unbalanced situations. Therefore, we propose a novel unidirectional power flow control algorithm with DVR maximum compensation limit consideration, which can effectively suppress problems of continuous rising in dc-link voltage. Progressive phase rotating method is applied to prevent compensated load voltage distortion or discontinuity. Appropriate and practical design of the dc storage capacitor's rating is also discussed. Simulation and experimental results for unbalanced voltage swell compensation are given to prove the validity and superior performance of the proposed algorithm.**

***Index Terms*—Energy storage, power control, power quality.**

I. Introduction

NOWADAYS, the proliferation and development of voltage-sensitive load equipment in diverse industries have been quick, such as automatic production lines, high-precision processing, computer centers, hospital equipments, and so on, their processes have also become much more vulnerable to degradation in the quality of power supply. Voltage quality problems in the form of voltage sags, voltage harmonics, and voltage swells can cause severe process disruptions, resulting in substantial economic and/or data losses [1], [2]. Dynamic voltage restorer (DVR) is a power electronic converter-based device, designed to protect critical loads from supply-side voltage disturbances. By inserting a voltage of desired magnitude and phase angle, it restores the load-side voltage to be a balanced, sinusoidal and nominal value, even when the source voltage is unbalanced or distorted. In addition, the DVR compensates for both steady-state and dynamic voltage quality problems, and is capable of generating or absorbing active and reactive power at its ac terminals [3], [4].

Manuscript received October 25, 2005; revised April 23, 2007. First published April 15, 2008; current version published September 24, 2008. Paper no. TPWRD-00626–2005.

C.-S. Lam and M.-C. Wong are with the Power Electronics Laboratory, Faculty of Science and Technology, University of Macau, Macao SAR, China (e-mail: cslam@umac.mo; c.s.lam@ieee.org; mcwong@umac.mo).

Y.-D. Han is with the Department of Electrical Engineering, Tsinghua University, Beijing, China, and also with the University of Macau, Macao SAR, China.

Color versions of one or more of the figures in this paper are available online at http://ieeexplore.ieee.org.

Digital Object Identifier 10.1109/TPWRD.2008.921142

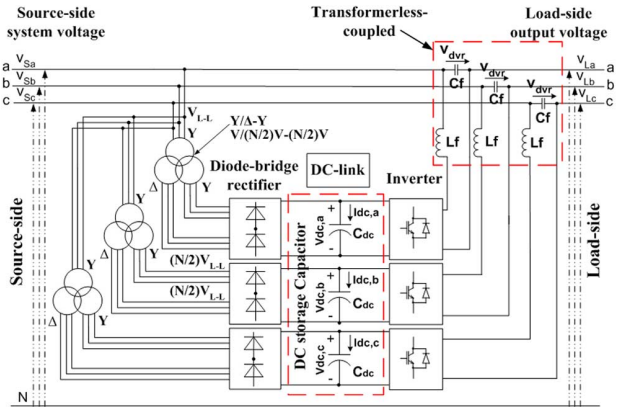

Fig. 1. Diode-bridge rectifier supported with transformerless-coupled DVR.

When the DVR is adopted in a low-voltage level distribution power network, a transformerless-coupled structure usually works better than the conventional transformer-coupled structure, as it eliminates the coupling transformer phase shift, voltage drop, harmonics loss, bulky size, expensive cost, and problems of saturation and inrush currents associated with the transformer magnetization phenomenon [5]. However, the use of a circuit configuration with three single-phase inverters and separated dc-link, as shown in Fig. 1, is indispensable for a transformerless-coupled DVR.

Installation of a diode-bridge rectifier circuitry to the DVR provides an economical means for the dc-link to negotiate active power. Unfortunately, this DVR configuration only allows unidirectional power flow from the diode-bridge rectifier circuitry to the inverter. When swell or overvoltage occurs in the power distribution lines, the conventional in-phase and phase-invariant voltage injection schemes [6], [7] cause inverters to absorb active power from the lines, which charges up the dc storage capacitors and increases their voltage levels. Excess dc-link voltage rise will damage the dc storage capacitors and switching devices. Moreover, the rise in dc-link voltage will nonlinearly increase switching loss [8] and lowers the DVR's system efficiency.

Because minimum energy scheme extracts the positive-sequence to achieve a three-phase minimum active power injection and absorption [1], [6], [7], its application will result in less fluctuation in dc-link voltage than in-phase and phase-invariant boosting methods under swell or overvoltage. Unfortunately,

unbalanced case may keep the DVR's one or two phases intake active power, which endangers the storage units and switching devices safety operations; as well as increasing switching loss. Thus, aborting the reverse flow of energy is an important issue that needs to be resolved. Many research studies in recent years focused on DVR energy optimization [1], [2], [6], [7] and different control methods [9]–[13], but unfortunately, there has not been further research investigating the voltage swell and overvoltage compensation problems existing in the DVR transfomerless-coupled strucutre for practical applications. Based on this limitation in the existing literatures, this paper aims at finding a solution to reverse power flow problems under unbalanced swell and overvoltage conditions.

Given that most of the loads in the power system are inductive, the follow discussion and analysis only focus on inductive loads. The main contribution of this paper on the DVR unidirectional power flow control algorithm is described in Section II, followed by a verification of the effectiveness of the proposed control algorithm with simulation and experimental results presented in Section III.

II. Proposed Unidirectional Power Flow Control Algorithm

In this section, the determination of the three-phase necessary rotating compensation angle is introduced in Section II-A. Since the calculated three-phase rotating compensation angle is restricted by the DVR's maximum compensation limit; its maximum compensation limit should also be considered within the proposed control algorithm, and details of this consideration are presented in Section II-B. After the calculation of the three-phase system voltage rotating compensation angle and the three-phase rotating compensation limit, the three-phase reference rotating compensation angle can be found in Section II-C. In order to prevent compensated load voltage distortion or discontinuity, the progressive phase rotating scheme is applied, as described in Section II-D. In Section II-E, the transformerless-coupled DVR system dc-link safety operation issue is examined. Finally, the control block diagram of the proposed unidirectional power flow control algorithm is illustrated in Section II-F.

A. Three-Phase Rotating Compensation Angle

The three-phase system voltages are assumed to have different phase shifts, so that an unbalanced phenomenon during unbalanced swell faults can be studied in the following manner. In Fig. 2(a), $\vec{V}_{si,pre-swell}$ represents the preswell system voltage phasor, $\vec{V}_{si,swell}$ represents the swell system voltage phasor, $\vec{I}_{Li}$ represents the load current phasor, with subscript $i = a$, b or c representing the corresponding phase, respectively.

Fig. 2(b) shows a three single-phase rotating compensation phasor diagram for Fig. 2(a). Considering the fundamental positive sequence in the following analysis, where subscript "1" represents the fundamental component. Before voltage swell, $\vec{V}_{si1,pre-swell}$ is equal to the load output voltage $\vec{V}_{oi1}$. With the assumption of constant load power angle $\varphi_{1,i}$, counterclockwise rotating direction is positive and clockwise rotating direction is negative. For calculation simplicity, because rotating $\vec{V}_{oi1}$ in a clockwise direction is the same as rotating $\vec{V}_{si1,swell}$ in a counterclockwise direction and vice versa, it has been assumed that

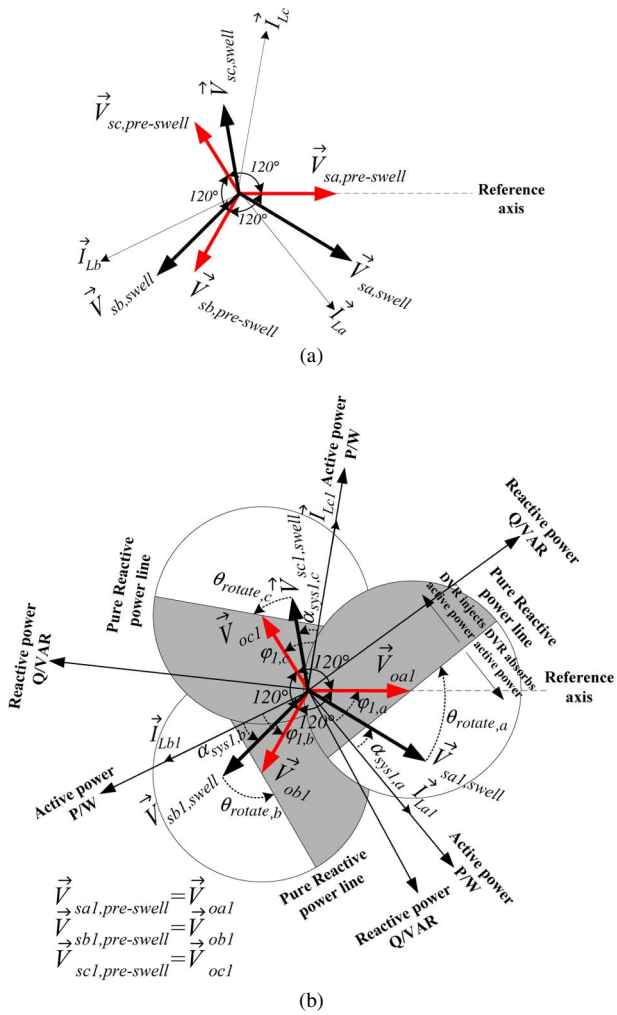

Fig. 2. (a) Unbalanced three-phase swell system voltages during unbalanced swell faults. (b) Three single-phase rotating compensation phasor diagram during swell.

$\vec{V}_{si1,swell}$ is rotated, and $\vec{V}_{oi1}$ is stationary. The location $\vec{I}_{Li1}$ is determined by $\vec{V}_{oi1}$ and thus it is also a stationary phasor. At the same time, the vertical y-axis can be considered as the reactive power (Q/VAR) axis when locating $\vec{I}_{Li1}$ onto the horizontal active power (P/W) x-axis. The middle line of each cycle represents pure reactive power line, which separates the DVR into active power injection and absorption regions. Each shaded or white semicircle area represents DVR active power injection or absorption region for each phase, respectively.

When the magnitude of $\left|\vec{V}_{si1,swell}\right|$ is larger than that of $\left|\vec{V}_{oi1}\right|$ and the DVR is absorbing active power, the single-phase necessary rotating compensation angle $\theta_{rotate,i}$ from the $\left|\vec{V}_{si1,swell}\right|$ location onto the pure reactive power line is

$$\theta_{rotate,i} = \cos^{-1}\left(\frac{\left|\vec{V}_{oi1}\right|\cos(\varphi_{1,i})}{\left|\vec{V}_{si1,swell}\right|}\right) - \alpha_{sys1,i} \qquad (1)$$

where $\alpha_{sys1,i}$ represents the phase angle difference between $\vec{V}_{si1,swell}$ and $\vec{I}_{Li1}$.

When the DVR's one, two or even three-phase system voltage phasors are located in the active power absorption regions, three

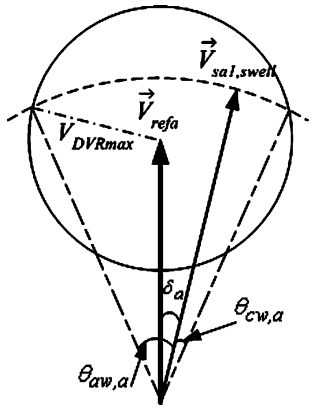

Fig. 3. Phase a rotating angle limit.

single-phase necessary rotating angle $\theta_{rotate,a}$, $\theta_{rotate,b}$, and $\theta_{rotate,c}$ can be calculated using (1). After that, the three-phase rotating compensation angle θ_{rotate} to suppress power intake by the dc storage capacitors can be chosen by as follows:

$$\theta_{rotate} = \max(\theta_{rotate,a}, \theta_{rotate,b}, \theta_{rotate,c}). \tag{2}$$

If the three-phase swell system voltage common rotating direction is counterclockwise, the three-phase swell system voltage rotating angle is $\theta_{r,system} = \theta_{rotate}$; otherwise $\theta_{r,system} = -\theta_{rotate}$in the clockwise rotating direction.

Although the three-phase rotating compensation angle control algorithm can suppress the continuous rise in dc storage capacitor voltage and provide a unidirectional power flow from the storage capacitor to the distribution system, the rotating angle $\theta_{r,system}$ is sometimes restricted by the DVR's maximum compensation limit $V_{DVR\max}$. Therefore, $V_{DVR\max}$ should also be considered within the rotating angle calculation process.

B. Three-Phase Rotating Compensation Limit

The three-phase rotating compensation angle may require DVR to inject voltage outside its maximum compensation limit. Thus the DVR's possible and allowable rotating angle range under $V_{DVR\max}$ has to be examined. Fig. 3 demonstrates the calculation of possible rotating angle range in each phase (also works for voltage sag case). With phase a as an example, $\vec{V}_{sa1,swell}$ is supposed to have a phase shift with the reference load voltage phasor $\vec{V}_{refa}$ by δ_a, then the DVR's compensation range can be illustrated by drawing a circle with radius $V_{DVR\max}$, and center at $\vec{V}_{refa}$. $\theta_{cw,a}$ and $\theta_{aw,a}$ represent the system voltage allowable rotating angle range in clockwise and counterclockwise direction, respectively. Subscripts *cw* and *aw* indicate clockwise and counterclockwise directions.

Similarly, by setting counterclockwise and clockwise rotating directions as positive and negative in Fig. 3, the three-phase clockwise and counterclockwise rotating angle limit under the DVR's maximum compensation limit can be calculated as [14]

$$\theta_{cw,a} = \delta_a - \cos^{-1} \times \left(\frac{\left|\vec{V}_{sa1,swell}\right|^2 + \left|\vec{V}_{refa}\right|^2 - V_{DVR\max}^2}{2\left|\vec{V}_{refa}\right|\left|\vec{V}_{sa1,swell}\right|} \right) \tag{3}$$

$$\theta_{aw,a} = \delta_a + \cos^{-1} \times \left(\frac{\left|\vec{V}_{sa1,swell}\right|^2 + \left|\vec{V}_{refa}\right|^2 - V_{DVR\max}^2}{2\left|\vec{V}_{refa}\right|\left|\vec{V}_{sa1,swell}\right|} \right). \tag{4}$$

From (3) and (4), the possible system voltage rotating range θ can be expressed as $\theta_{cw,a} \le \theta \le \theta_{aw,a}$. Applying this conclusion to the three-phase system, the three-phase rotating compensation limit is necessary to fulfill

$$\theta_{cw} \le \theta \le \theta_{aw} \tag{5}$$

where

$$\theta_{cw} = \max(\theta_{cw,a}, \theta_{cw,b}, \theta_{cw,c});$$
$$\theta_{aw} = \min(\theta_{aw,a}, \theta_{aw,b}, \theta_{aw,c})$$

The previous calculated three-phase system voltage rotating compensation angle $\theta_{r,system}$ can be inside or outside the rotating compensation limit, which can be divided into two situations for the analysis:

Situation One: $\theta_{cw} \le \theta_{r,system} \le \theta_{aw}$, if $\theta_{r,system}$ falls inside the rotating compensation limit, $\theta_{r,system}$ will be the common rotating angle for the three-phase system voltage.

Situation Two: $\theta_{r,system} > \theta_{aw}$ or $\theta_{r,system} < \theta_{cw}$, this is used when the system voltage falls outside the rotating compensation limit; selecting either θ_{cw} or θ_{aw} to be $\theta_{r,system}$ can be a compromised solution. However, this situation still causes the DVR to absorb active power from the system. Because the degree of dc-link voltage rise still has the potential to damage the dc storage capacitors and/or switching devices, remedies will be proposed in Section II-E.

C. Final Three-Phase Reference Rotating Angle

In parts A and B, it has been assumed $\vec{V}_{si1,swell}$ is rotated and $\vec{V}_{oi1}$ is a stationary phasor. In contrast, in practical situations $\vec{V}_{si1,swell}$ is stationary while $\vec{V}_{oi1}$ rotates by changing the DVR inject voltage phase angle. In addition, the inject voltage phase angle varies by rotating the DVR reference voltage angle. Therefore, the final three-phase reference load voltage rotating angle will be

$$\theta_{r,ref} = -\theta_{r,system}. \tag{6}$$

In reality, rotating the reference load voltage angle has no impact on the system voltage harmonics, negative sequence or zero sequence compensation. It only changes the DVR's compensating voltage positive sequence phase angle. In addition, system voltage harmonics, negative sequence and zero sequence components are compensated by the balanced and sinusoidal

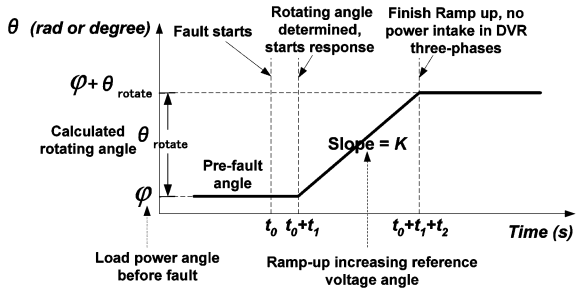

Fig. 4. Progressive phase rotating process.

reference load voltage. As a result, the three-phase load output voltage remains balanced after angle rotation.

D. Progressive Phase Rotating Method

After calculating the three-phase reference rotating angle, the change of load voltage phase angle can be taken immediately to provide unidirectional power flow to the DVR. However, the instantaneous step change of phase angle will cause the load voltage wave-shape discontinuity, inaccurate voltage zero-crossing and load power swing. This may be detrimental to sensitive loads [6]. It is also well known that loads such as adjustable speed drives are particularly sensitive to deviations in either voltage magnitude or phase angle jump. To alleviate this problem, a progressive phase rotating scheme can be applied for smooth transition of the load voltage. When swell or overvoltage fault clearance occurs, this rotating method should also be applied to recover the original three-phase load voltage phase angle.

The progressive phase rotating process is shown in Fig. 4. Only the ramp-up of the phase angle from normal state to swell or overvoltage state in inductive loads is illustrated. Changes from the swell or overvoltage state back to the normal state can be considered as a ramp-down process. In order to prevent discontinuity in the voltage waveform, the reference load voltage starts to ramp-up or ramp-down at a slope of K or $-K$. However, the ramp-up/ramp-down process implies that the frequency will change slightly. Unfortunately, slight variations in frequency on an electric system can cause severe damage to generator and turbine shafts due to the large torques developed subsequently [15]. If a frequency variation tolerance $\pm\Delta f$ is defined for a sensitive load, the ramp-up/ramp-down slope of the phase rotating process is restricted by

$$|K| < 2\pi\Delta f \tag{7}$$

where $t_2 =$ total phase angle rotating time.

E. DC-Link Safety Operation Issue

Based on the previous parts, the proposed control algorithm has the ability to suppress the dc-link voltage rise problems, and to provide the DVR with unidirectional power flow under voltage swell or overvoltage situation. Unfortunately, when a large energy swell happens, the control system requires time to sample, take calculation, and perform controlling. At the same time, in order to prevent the load voltage distortion or discontinuity, the phase of the inject voltage has to be changed progressively, making it unavoidable for the DVR to absorb active power shortly. Therefore, the possibility for the dc-link voltage level rise still exists. With appropriate design of the dc capacitor voltage rating and the application of the proposed control algorithm, it can provide a more reliable environment for the dc-link safety operation.

Assuming the transient of swell fault is short, the power absorption during transient is small and can be neglected. During the steady-state swell duration, the swell system and load voltages are assumed to be sinusoidal; and fundamental component dominates the power calculation.

From Fig. 4, the total phase angle rotating time is

$$t_2 = \frac{\theta_{rotate}}{K}. \tag{8}$$

If P_{in}, P_{out}, and P_{DVR_loss} are the input power from the source, the load power and the DVR system power loss, respectively, the integration of the dc storage capacitor power absorption p_{dc} within a period of time $(t_1 + t_2)$ is

$$\int_{t_0}^{t_0+t_1+t_2} p_{dc}(\tau)\,d\tau = \int_{t_0}^{t_0+t_1+t_2} (P_{in} - P_{out} - P_{DVR\_loss})d\tau \tag{9}$$

$$P_{in} = |V_{sys}|\,|I_L|\cos[\alpha(\tau)] \tag{10}$$

$$P_{out} = |V_o|\,|I_L|\cos(\varphi) \tag{11}$$

where $t_0 =$ time at swell moment, usually set $t_0 = 0$, $t_1 = (t_1 - t_0) =$ summation of DVR sampling time, control algorithm computational time and response time after swell fault; $|V_{sys}|$ represents the swell system voltage magnitude; $|V_o|$ represents the rated load output voltage magnitude; and $|I_L|$ represents the load current magnitude. $\alpha(\tau)$ is the load power angle φ before the progressive phase rotating process, $\alpha(\tau) = K(\tau - t_1) + \varphi$ is given during the progressive phase rotating process and the load power factor $\cos(\varphi) =$ constant .

For safety operation, the energy absorbed by the dc storage capacitor must restrict the dc-link voltage from exceeding its maximum rating, which yields

$$\int_{t_0}^{t_0+t_1+t_2} p_{dc}(\tau)\,d\tau \le \frac{C_{dc}}{2}\left[v_{dc\max}^2 - V_{dc0}^2\right] \tag{12}$$

where C_{dc} represents the dc storage capacitance; $v_{dc\max}$ represents the permitted maximum dc capacitor rating; V_{dc0} represents the dc capacitor operational voltage before swell; $V_{dc0} = \sqrt{3} \times N \times 1.35 \times |V_o|$; N and 1.35 are the transformer turn ratio and diode-bridge rectifier ratio, respectively.

For the worst case design of the dc capacitor rating, it is assumed that the DVR is a lossless system; load is pure resistive and it is operating at rated load voltage and current situation. Moreover, if the dc capacitor rating is designed under maximum

2 p.u. swell voltage compensation (a larger value than the definition of swell and overvoltage in [15]), it can provide the dc-link with a more reliable operating environment. From (9) and (12), the design case of the dc capacitor rating can be obtained, as shown in (13) at the bottom of the page.

Substituting the worst case rotating angle value $\theta_{rotate\,\max} = 60^\circ = \pi/3$ into (13) yields the minimum dc capacitor rating required

$$v_{dc\,\max} \geq \sqrt{\frac{2}{C_{dc}} |V_o|\,|I_L| \left[t_1 + \frac{0.68485}{K}\right] + (2.34N\,|V_o|)^2}. \tag{14}$$

For the design of minimum dc capacitor rating required in an 110 V/5 kVA DVR system, it is assumed $C_{dc} = 1650\ \mu$F, $t_1 = 50$ ms, and $N = 0.58$. Substituting them into (14) yields

$$v_{dc\,\max} \geq \sqrt{122288.1 + \frac{1369700.0}{K}}. \tag{15}$$

Based on (15), the required dc capacitor rating corresponding to different phase rotating speed K in the power lossless 110 V/5 kVA DVR system can be found. When K increases, there is less energy absorbed by the DVR during swell, thus the required $v_{dc\,\max}$ is also reduced. The required $v_{dc\,\max}$ is usually inversely proportional to K. Smaller $v_{dc\,\max}$ is beneficial because it lowers the DVR's initial cost. However, K is usually restricted by sensitive loads. Rotating speed that is too high will be detrimental to sensitive loads, when $K = 5$ rad/s, and $v_{dc\,\max} \geq 630$ V. However, when $K = 1.745$ rad/s (100°/s), $v_{dc\,\max} \geq 952$ V. In addition, for "phase" nonsensitive loads, the load voltage phase angle can be changed immediately ($|K| = \infty$), $v_{dc\,\max} \geq 350$ V.

Based on the worst case consideration, $v_{dc\,\max}$ respects to different K in different capacity and base voltage DVR system can be designed. In a practical case, because power loss always exists in the system, the lossless dc capacitor rating design (14) can provide greater dc storage capacitor safety margin.

Unfortunately, if the required compensating rotating angle $\theta_{r,\mathrm{system}}$ does not satisfy the three-phase rotating compensation limit $\theta_{cw} \leq \theta \leq \theta_{aw}$, it is also unavoidable that dc-link voltage level may rise. When the degree of the dc-link voltage rise remains large enough to damage the dc storage capacitors and/or switching devices, a discharge resistor or battery to the dc capacitor may be shunted. However, using resistor will increase system loss, decrease its efficiency, while using battery will increase the system's initial cost. As a result, connecting a discharge resistor or battery are two backup solutions to solve the unavoidable excess voltage rise problem when the swell is out of the compensation limit.

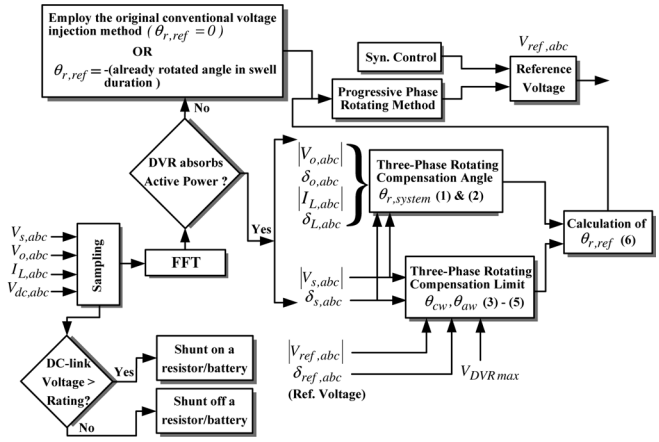

Fig. 5. Control block diagram for unidirectional power flow control algorithm.

F. Implementation of the Unidirectional Power Flow Control Algorithm

Fig. 5 shows the control block diagram for the proposed unidirectional power flow control algorithm. From Fig. 5, the three-phase system voltage, load output voltage, load current and dc-link voltage are sampled. With the appropriate design of the dc capacitor rating, if either one of the dc capacitor voltage has the possibility to exceed its maximum rating, a discharge resistor or battery can be shunted to the corresponding dc-link. If the dc capacitor voltage is lower than its rating, the resistor or battery is not connected. The magnitude and phase of the system voltage, load output voltage and load current are obtained by utilizing FFT. If the DVR is not absorbing active power, the three-phase reference load voltages either do not need angle rotation $\theta_{r,ref} = 0$, or require backward rotation during swell to recover the original three-phase load voltage phase angle before fault. Inversely, if either one phase is absorbing active power, the three-phase reference load voltage should be rotated one phase angle in order to move the DVR away from the active power absorption region. After the calculation of $\theta_{r,system}$ and θ_{cw}, θ_{aw} and $\theta_{r,ref}$ for three-phase can be determined. In order to have smooth transition of the load voltage, progressive phase rotating method is applied to change the reference voltage angle progressively. This will change the DVR's inject voltage phase angle, so that the DVR does not absorb active power from the system during swell fault. The reference signal should be synchronized with the fundamental positive-sequence of the system voltage.

III. Simulation and Experimental Results

Due to the minimum energy scheme can achieve the least active power flow of the dc-link compared with in-phase and

$$v_{dc\,\max} \geq \sqrt{\frac{2}{C_{dc}} |V_o|\,|I_L| \left[t_1 + \frac{2\sin(\theta_{rotate}) - \theta_{rotate}}{K}\right] + (2.34N\,|V_o|)^2}. \tag{13}$$

TABLE I
110 V/5 KVA DVR SYSTEM PARAMETERS

Test Parameters	Nominal Values
V_{phase}	$110V_{rms}$/50Hz
Filtering inductance L	7.6mH
Filtering capacitance C	11μF
DC-link storage capacitance C_{dc}	1650μF/900VDC
Transformer turn ratio N	0.58
Load	Balanced 30Ω (Power Factor =1)
Switching frequency f_s	10kHz
Progressive phase rotating speed K	100 degree/s or 1.745 rad/s

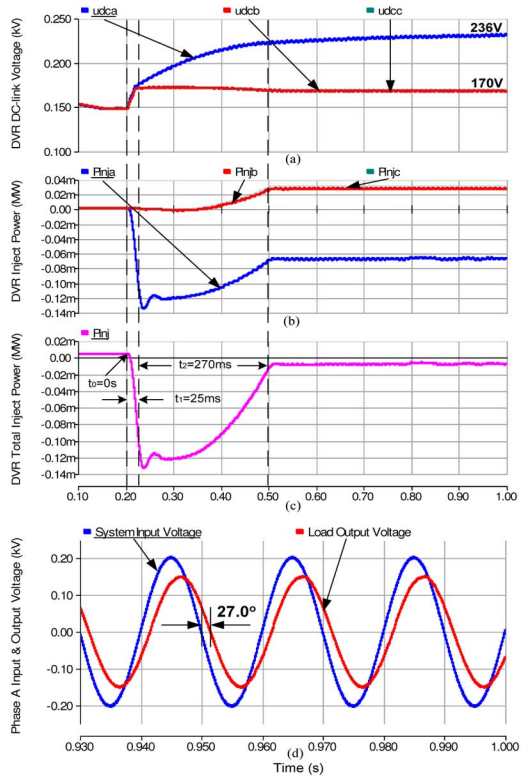

Fig. 6. Minimum energy injection scheme for unbalanced voltage swell compensation. (a) DVR dc-link voltage. (b) DVR inject power/phase. (c) DVR total inject power. (d) Phase a swell system and load output voltages.

phase-invariant schemes [6], [7], the in-phase and phase-invariant schemes will not be discussed in this paper. In this section, only representative simulation and experimental results of minimum energy scheme and the proposed control algorithm are included to highlight the proposed algorithm's superior unbalanced swell and overvoltage compensation capability over the three conventional schemes.

A multiloop control scheme is employed for this DVR system and its block diagram representation can be found in [4]. Table I shows the 110 V/5 kVA DVR system parameters for the simulations and experiments.

Since the DVR absorbs pure active power under pure resistive load, this worst case situation under unbalanced voltage swell compensation is chosen for the following simulation and experimental verifications.

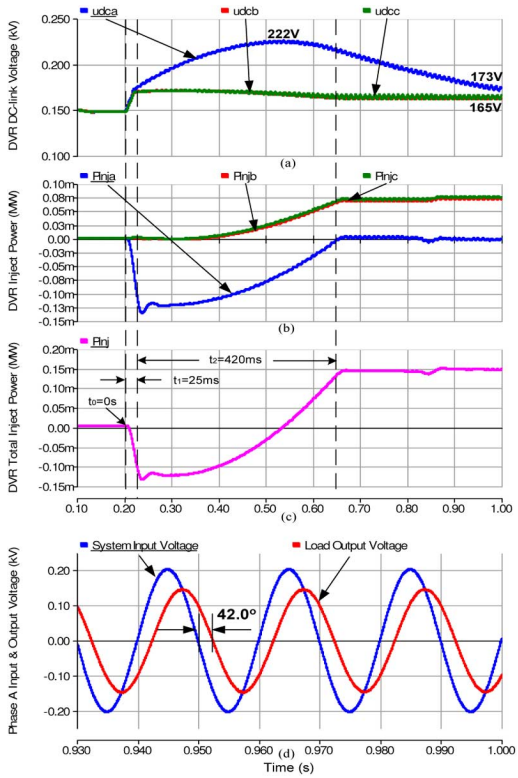

Fig. 7. Proposed unidirectional power flow control algorithm for unbalanced voltage swell compensation. (a) DVR dc-link voltage. (b) DVR inject power/phase. (c) DVR total inject power. (d) Phase a swell system and load output voltages.

A. Simulation Results

Simulation studies were carried out using PSCAD/EMTDC. In the simulation, phase a system voltage meets 30% swell at 0.2 s with a duration of 0.8 s, while the other two phases remain unfaulted. The simulation results for minimum energy scheme and the proposed control algorithm can be illustrated clearly in Figs. 6 and 7, respectively. Due to collection of the sample and process computations, the minimum energy scheme and the proposed control algorithm start to have response after $t_1 = 25$ ms of the swell fault.

Fig. 6 shows the compensation results of using the minimum energy scheme. Even though Fig. 6(c) indicates that the DVR's total inject power curve is close to zero after 0.50 s, phase a still absorbs active power of 67.0 W, as illustrated in Fig. 6(b). In addition, phases b and c are injecting active power. Therefore, phase a dc-link voltage continues to rise as indicated in Fig. 6(a), and it finally reaches 236 V at the end of simulation. As a result, minimum energy scheme may not be capable to solve the problems of continuous rising in dc-link voltage under unbalanced swell situation. Fig. 6(b) and (c) also shows the required $t_2 = 270$ ms. Fig. 6(d) demonstrates that the swell system and load output voltages will have a phase angle difference of 27.0° after applying this scheme.

Next, the proposed control algorithm is applied to the unbalanced swell simulation. From Fig. 7(b) and (c), phase a inject power and total inject power curves progressively rise until phase a inject power is close to zero. In the mean time, the increasing speed of phase a dc-link voltage falls progressively.

At 0.65 s, even though phase a does not absorb active power from the system, its dc-link voltage has not yet recovered to the voltage level of phases b and c. This is because phase a total energy absorption is not yet zero at that moment. When phase a total energy absorption during swell is nearly zero, its dc-link voltage will drop back to the voltage level as phases b and c, which is shown in Fig. 7(a). Phase a dc-link voltage has a maximum value of 222 V (236 V for minimum energy method) during swell duration. Fig. 7(b) and (c) shows the required $t_2 = 420$ ms. Fig. 7(d) demonstrates that the swell system and load output voltages require at least a phase angle difference of 42.0° to prevent active power absorption of the DVR. Figs. 6(d) and 7(d) show that load voltage can both be compensated to the nominal 110 $V_{\rm rms}$. Compared with Figs. 6(a), 7(a) clearly illustrates the effectiveness of the proposed control algorithm in solving problems of unbalanced voltage swell and overvoltage compensation.

B. Experimental Results

In order to verify the simulation results, a detailed experimental investigation of the DVR system was carried out in the laboratory. Fig. 1 shows the circuit configuration of the transformerless-coupled DVR experimental prototype. The control system of the prototype is a digital signal processor (DSP) TMS320 C32. The sampling frequency of the system is set at 6.4 kHz. In the experiment, a 30% single-phase (phase a) swell is generated (nominal voltage is 110 $V_{\rm rms}$). Due to the collection of samples and process computations of the DSP, the minimum energy scheme and the proposed control algorithm start to have response after $t_1 = 50$ ms of the swell or overvoltage phenomenon in the experimental prototype.

Figs. 8 and 9 depict the experimental results for a 30% unbalanced (phase a) swell in using minimum energy and the proposed control methods, respectively. Although Fig. 8(c) shows that the DVR's total inject power curve is close to zero after 36.03 s, phase a still absorbs active power of about 85 W, as illustrated in Fig. 8(b). Therefore, phase a dc-link voltage continues to rise as indicated in Fig. 8(a), and it rises to 251.6 V after 1.28 s voltage swell duration. Thus, the danger for the dc storage capacitors, switching devices, and also the large switching loss still exist. As a result, the experimental results provide good evidence that the minimum energy scheme cannot solve problems of continuous rising in dc-link voltage under unbalanced swell or overvoltage situation. Fig. 8(b) and (c) show the required $t_2 = 245$ ms. Fig. 8(c) demonstrates that the swell system and load output voltages will have a phase angle difference of 23.8° after applying the minimum energy scheme. The load output voltage can be compensated to the nominal 110 $V_{\rm rms}$.

Fig. 9(b) and (c) shows that the swell happens at 39.83 s. When the proposed control algorithm starts working at 39.88 s, the DVR's three-phase inject power and its total inject power curves progressively rise until phase a inject power is close to zero (after 40.26 s). At the same time, its dc-link voltage level progressively decreases until it resumes the voltage level as un-swell phases b and c, as illustrated in Fig. 9(a). During the unbalanced voltage swell, phase a dc-link voltage has a maximum value of 212.1 V (251.6 V for minimum energy method). Fig. 9(b) and (c) also shows the required $t_2 = 385$ ms. Fig. 9(c) demonstrates that the swell system and load output voltages require at least a phase angle difference of 40.2° to prevent DVR's active power absorption. The load output voltage can also be compensated to the nominal 110 $V_{\rm rms}$.

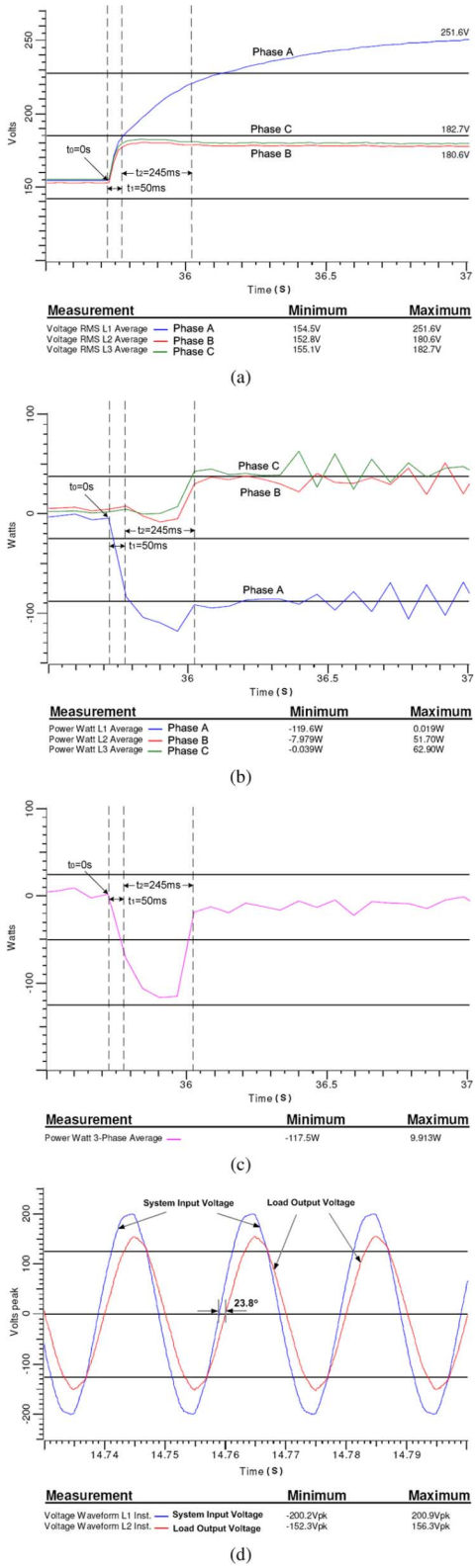

Fig. 8. Minimum energy injection scheme for unbalanced voltage swell compensation. (a) DVR dc-link voltage. (b) DVR inject power/phase. (c) DVR total inject power. (d) Phase a swell system and load output voltages.

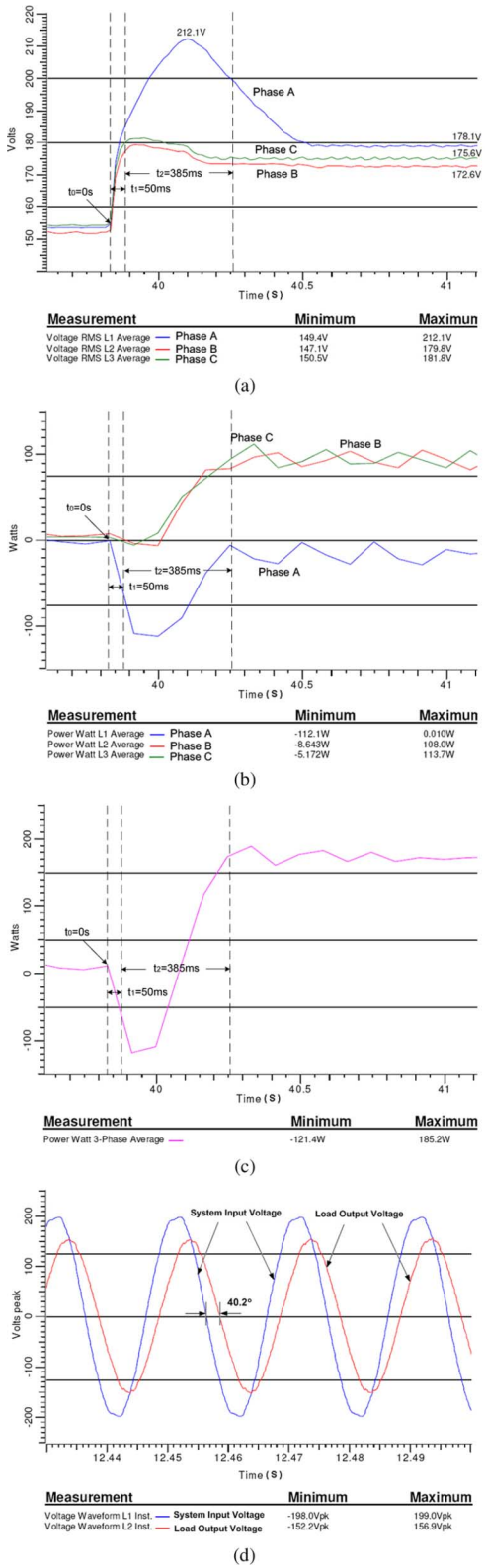

Fig. 9. Proposed unidirectional power flow control algorithm for unbalanced voltage swell compensation. (a) DVR dc-link voltage. (b) DVR inject power/phase. (c) DVR total inject power. (d) Phase a swell system and load output voltages.

Experimental findings shown in Figs. 8 and 9 are consistent with the simulation results shown in Figs. 6 and 7. This proves that the minimum energy scheme cannot be capable of protecting the energy storage units and switching devices' safety operation under unbalanced swell or overvoltage situations. Further, it can create a larger switching loss to the DVR. These results clearly illustrate and verify the effectiveness and superior performance of the proposed control algorithm in solving the reverse power flow problems under swell or overvoltage situation.

IV. Conclusion

This paper illustrates the voltage swell and overvoltage problems in a diode-bridge rectifier supported transformerless-coupled DVR. Among the three conventional voltage injection schemes, the minimum energy compensation scheme can solve part of the problems during balanced case, by absorbing the least active power during swell or overvoltage. Unfortunately, it cannot handle those problems associated with the rise in dc-link voltage during unbalanced situation.

To restrict the dc-link voltage from exceeding its safe operational range and reduce switching loss, a novel unidirectional power flow control algorithm is proposed. With a DVR maximum compensation limit, progressive phase rotating speed and dc-link safety operation considerations, the proposed control algorithm can solve reverse power flow problems in both balanced and unbalanced swell or overvoltage situations, while the compensated load output voltage remains balanced, sinusoidal and at a nominal value.

For both minimum energy scheme and our proposed scheme, they require at least one system frequency cycle sampling data to get the phase angle from the fast Fourier transform (FFT). Moreover, due to the collection of samples and other process computations for both schemes by DSP, the response time of the DVR is extended. To deal with this limitation, we had suggested an appropriate design of the dc-link rating as discussed in Section II-E (energy absorbed during DSP processing time is under consideration).

To conclude, simulation and experimental results for unbalanced voltage swell compensation are given to prove the validity of the proposed control algorithm and demonstrate superior compensation performance, compared to the conventional minimum energy scheme.

Acknowledgment

The authors would like to thank the Research Committee of the University of Macau and the Flexible AC Transmission and Distribution System Research Institute of Tsinghua University for their helpful comments and support.

References

[1] D. M. Vilathgamuwa, A. A. D. R. Perera, and S. S. Choi, "Voltage sag compensation with energy optimized dynamic voltage restorer," *IEEE Trans. Power Del.*, vol. 18, no. 3, pp. 928–936, Jul. 2003.

[2] D. M. Vilathgamuwa, A. A. D. R. Perera, S. S. Choi, and K. J. Tseng, "Control of energy optimized dynamic voltage restorer," in *Proc. IEEE IECON'99*, 1999, vol. 2, pp. 873–878.

[3] A. Ghosh and G. Ledwich, "Compensation of distribution system voltage using DVR," *IEEE Trans. Power Del.*, vol. 17, no. 4, pp. 1030–1036, Oct. 2002.

[4] C.-S. Lam, M.-C. Wong, and Y.-D. Han, "Stability study on dynamic voltage restorer (DVR)," in *Proc. IEEE ICPESA'04*, 2004, pp. 66–71.
[5] B. H. Li, S. S. Choi, and D. M. Vilathgamuwa, "Transformerless dynamic voltage restorer," *Proc Inst. Elect. Eng. Gener. Transm. Distrib.*, vol. 149, pp. 263–273, May 2002.
[6] S. S. Choi, B. H. Li, and D. M. Vilathgamuwa, "Dynamic voltage restoration with minimum energy injection," *IEEE Trans. Power Syst.*, vol. 15, no. 2, pp. 51–57, Feb. 2000.
[7] S. Polmai, T. Ise, and S. Kumagai, "Experiment on voltage sag compensation with minimum energy injection by use of a micro-SMES," in *Proc. IEEE PCC'02*, 2002, vol. 2, pp. 415–420.
[8] G. C. D. Sousa, B. K. Bose, J. Cleland, R. J. Spiegel, and P. J. Chappell, "Loss modeling of converter induction machine system for variable speed drive," in *Proc. IEEE IECON'92*, 1992, vol. 1, pp. 114–120.
[9] A. Elnady and M. M. A. Salama, "Mitigation of voltage disturbances using adaptive perceptron-based control algorithm," *IEEE Trans. Power Del.*, vol. 20, pp. 309–318, Jan. 2005.
[10] J. G. Nielsen, F. Blaabjerg, and N. Mohan, "Control strategies for dynamic voltage restorer compensating voltage sags with phase jump," in *Proc. IEEE APEC'01*, 2001, vol. 2, pp. 1267–1273.
[11] M. J. Newman, D. G. Holmes, J. G. Nielsen, and F. Blaabjerg, "A dynamic voltage restorer (DVR) with selective harmonic compensation at medium voltage level," in *Conf. Rec. IEEE-IAS Annu. Meeting*, 2003, vol. 2, pp. 1228–1235.
[12] M. Vilathgamuwa, A. A. D. R. Perera, and S. S. Choi, "Performance improvement of the dynamic voltage restorer with closed-loop load voltage and current-mode control," *IEEE Trans. Power Electron.*, vol. 17, no. 5, pp. 824–834, Sep. 2002.
[13] H. Kim and S.-K. Sul, "Compensation voltage control in dynamic voltage restorers by use of feed forward and state feedback scheme," *IEEE Trans. Power Electron.*, vol. 20, no. 5, pp. 1169–1177, Sep. 2005.
[14] C. Yang, W. X. Ma, and Y. D. Han, "Studies on the Series Power Quality Controller," Ph.D. dissertation, Elect. Eng. Dept., Tsinghua Uni., Beijing, China, 2002.
[15] *IEEE Recommended Practice on Monitoring Electric Power Quality*, , 1995, IEEE Standard 1159:1995.

Chi-Seng Lam (S'04–M'08) received the B.Sc. and M.Sc degrees in electrical and electronics engineering from the University of Macau (UM), Macao SAR, China, in 2003 and 2006, respectively.

From September 2003 to September 2006, he was working full-time in a research group at the Power Electronics Laboratory of UM. He is currently working in the Campus Development and Engineering Section (CDE) at UM. He is also a part-time researcher at the Power Electronics Laboratory of UM. His research interests include power electronics, power quality, and DFACTS.

Mr. Lam received the Macao Foundation Postgraduate Research Scholarship in 2003–2005. He also received the Third Regional Inter-University Postgraduate Electrical and Electronic Engineering Conference (RIUPEEEC) Merit Paper Award in 2005.

Man-Chung Wong (SM'06) received the B.Sc. and M.Sc degrees in electrical and electronics engineering from the University of Macau, in 1993 and 1997, respectively, and the Ph.D. degree from the Tsinghua University, Beijing, China, in 2003.

He has been a Lecturer in the Department of Electrical and Electronics Engineering, University of Macau, since 1998. He has been an Assistant Professor at the University of Macau since 2003. His research interests are FACTS and DFACTS, power quality, custom power, and PWM.

Dr. Wong received the Young Scientist Award from the "Instituto Internacional De Macau" in 2000, the Young Scholar Award from the University of Macau in 2001, and second prize of the 2003 Tsinghua University Excellent Ph.D. thesis award.

Ying-Duo Han (SM'91) was born in Shenyang, Liaoning province, China, in 1938. He received the B.S. and M.S. degrees from the Electrical Engineering Department, Tsinghua University, Beijing, China, in 1962 and 1965, respectively, and the Ph.D. degree from Erlangen-Nuerenberg University, Erlangen, Germany.

He is a Professor in the Electrical Engineering Department, Tsinghua University, and he was the Vice-Chairman and Chairman of the Electrical Engineering Department from 1986 to 1995. Since 1989, he has been the head of Power Electronics Research Center, Tsinghua University. He is a Visiting Professor at the University of Macau, China. He has published two books and more than 100 papers. For more than 30 years, he has been involved in education and research work on electric power systems and the automation field. In recent years, he has been involved in research on FACTS and DFACTS, intelligent control, regional stability control, new dynamic security estimation, and control based on GPS.

Dr. Han received four State-level prizes, and six first and second ranked Province-level and Ministry-level prizes. He is a Member of Chinese Academy of Engineering.